NANO LETTERS

Letter

pubs.acs.org/NanoLett

Out-of-Plane Reflection and Refraction of Light by Anisotropic Optical Antenna Metasurfaces with Phase Discontinuities

Francesco Aieta,[†,‡] Patrice Genevet,[†,§] Nanfang Yu,[†] Mikhail A. Kats,[†] Zeno Gaburro,[†,∥] and Federico Capasso*[,†]

[†]School of Engineering and Applied Sciences, Harvard University, Cambridge, Massachusetts 02138, United States

[‡]Dipartimento di Fisica e Ingegneria dei Materiali e del Territorio, Università Politecnica delle Marche, via Brecce Bianche, 60131 Ancona, Italy

[§]Institute for Quantum Studies and Department of Physics, Texas A&M University, College Station, Texas 77843, United States

[∥]Dipartimento di Fisica, Università degli Studi di Trento, via Sommarive 14,38100 Trento, Italy

Supporting Information

ABSTRACT: Experiments on ultrathin anisotropic arrays of subwavelength optical antennas display out-of-plane refraction. A powerful three-dimensional (3D) extension of the recently demonstrated generalized laws of refraction and reflection shows that the interface imparts a tangential wavevector to the incident light leading to anomalous beams, which in general are noncoplanar with the incident beam. The refracted beam direction can be controlled by varying the angle between the plane of incidence and the antenna array.

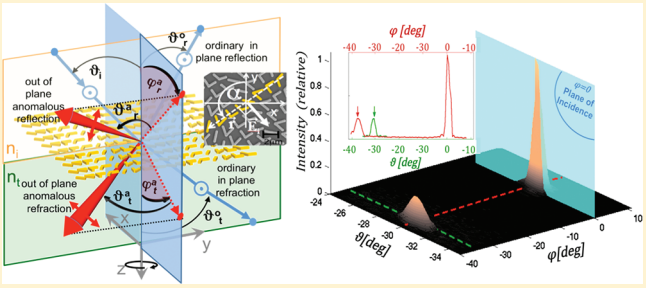

KEYWORDS: *Plasmonics, optical antenna, metasurfaces, reflection, phase discontinuities, Snell's Law*

Reflection and refraction are two of the most common phenomena in classical optics and are governed by well-established and simple laws, regarded so far as immutable, which can be derived in a straightforward and elegant way using the stationary phase principle.[1−4] A key feature of these laws is that the incident, reflected, and transmitted beams lie in the same plane, that is, the plane of incidence. Recent research on metamaterials and in particular on left-handed optical materials has shown that even if light can be refracted in unusual ways,[5−8] the refraction angle is still described by the traditional form of Snell's law, albeit with a negative index of refraction.[9−11]

Optical antennas have enabled the control of the electromagnetic radiation at the nanometric scale[12,13] and have found a large number of applications ranging from light emitters for applications in LEDs,[14] lasers,[15] or polarization control devices[16] to receivers in nanoimaging, spectroscopy, and photovoltaics.[17−20] By patterning an array of optical antennas on a dielectric substrate, we have recently been able to create a new class of metasurfaces that can be used to fully control light in direction, shape of the wavefront, and polarization by local control of the phase and amplitude response of the antennas.[21] Such plasmonic interfaces are promising for a new type of flat and small foot print photonics devices.[21−23]

In particular in our previous work we showed that designer nanometric thick plasmonic interfaces consisting of arrays of varying shape and size V-antennas with constant phase gradient oriented parallel the plane of incidence, modify the direction of reflected and refracted mid-infrared light, which now obeys a generalization of the traditional laws of reflection and refraction.[21] This work has been extended to the near-infrared wavelength range using arrays of suitably scaled down V-antennas.[24]

In the present work, performed on the same structures, we have discovered a new effect: a rotation of the plane of incidence by an arbitrary angle with respect to the phase gradient leads to noncoplanar refraction. Remarkably, this anomalous tailorable refraction can be described in terms of a generalized Snell's law in three-dimension (3D). Similarly we obtain a generalized law of reflection that also leads to out-of-plane beaming, when the phase gradient forms an angle with the plane of incidence. New critical angles for refraction and reflection are derived (see Supporting Information).

We point out that out-of-plane refraction was previously theoretically proposed but in a completely different context.[25] That work considered the reflection and refraction of inhomogeneous waves, that is, waves having a complex value for the tangential component of the incident wavevector. Similar out of plane beaming effects have been reported in 3D photonic crystals with anisotropic band structures,[26,27] but in this case the effect results from propagation in a 3D anisotropic medium rather than from anomalous reflection and refraction at an interface.

Received: January 17, 2012
Revised: February 13, 2012
Published: February 15, 2012

   dx.doi.org/10.1021/nl300204s | Nano Lett. 2012, 12, 1702−1706

In its modern formulation known as principle of stationary phase,[1] Fermat's principle describes with a simple formalism the fact that the actual path taken by a light ray from one point to another maximizes the constructive interference between its neighboring optical paths, that is, the variation of the accumulated phase is zero with respect to an infinitesimal variation of the path. We use the stationary phase principle to derive the reflection and refraction laws for plane waves at interfaces with constant phase gradients oriented along an arbitrary direction with respect to the plane of incidence.

The stationary phase principle applied to the two infinitesimally close paths magenta and green in Figure 1a

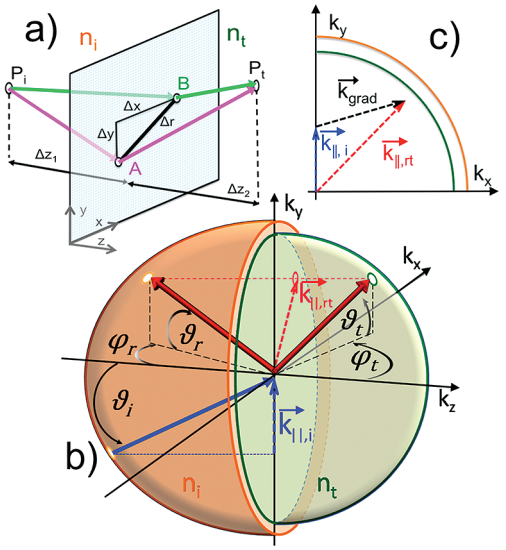

Figure 1. Schematics used to describe the generalized refraction at an interface with arbitrary orientation of the phase gradient and the associated k-space representation. (a) The interface between two media of refractive index n_i and n_t is structured to introduce a constant phase gradient $\overrightarrow{d\Phi}/dr$ along the line connecting points A and B which are assumed to be very close. We consider two points, one in medium 1 and one in medium 2 (P_i and P_t), and following the stationary phase principle principle, we set equal to zero the difference of the phase accumulated along the two infinitesimally close paths separated by a distance Δr. (b,c) The plane of incidence is oriented in such a way that the projection of the incident wave-vector on the interface ($\vec{k}_{\|,i}$) forms a nonzero angle with the direction of the phase gradient. As a result during the interaction with the plasmonic interface, the light beam acquires a k-vector component parallel to the interface equal to the phase gradient ($\vec{k}_{\|,rt} = \vec{k}_{\|,i} + \vec{k}_{grad}$) that gives rise to the out of plane anomalously reflected and refracted beams.

imposes that $\int_A \varphi(\vec{r})d\vec{r} = \int_B \varphi(\vec{r})d\vec{r}$, where the integrals are along the paths through point A and B, respectively, which can be rewritten as

$$\left[\int_{P_i}^{A} \vec{k}_i \cdot d\vec{r} - \int_{P_i}^{B} \vec{k}_i \cdot d\vec{r}\right] + \left[\int_{A}^{P_t} \vec{k}_t \cdot d\vec{r} - \int_{B}^{P_t} \vec{k}_t \cdot d\vec{r}\right] + \frac{\overrightarrow{d\Phi}}{dr}(\vec{r}_A - \vec{r}_B) = 0 \quad (1)$$

where $\vec{k}_i(\vec{k}_t)$ is the wavevector of light in the medium of index n_i (n_t) and $\vec{r}_{A(B)}$ is the position of A (B) along the surface. For constant phase gradients, the accumulated phase of rays intersecting the interface is a convex downward function for all values of x and y,[2] so we can rewrite the stationary phase condition in eq 1 for the x and y spatial coordinate independently. After integration, one obtains the expressions for the parallel components of the wavevector of the refracted beam

$$\begin{cases} k_{x,t} = k_{x,i} + \dfrac{d\Phi}{dx} \\ k_{y,t} = k_{y,i} + \dfrac{d\Phi}{dy} \end{cases} \quad (2)$$

Note that due to the lack of translational invariance along the interface the tangential wavevector of the incident photon is not conserved; the interface contributes an additional "phase matching" term equal to the phase gradient, which allows one to control the direction of the reflected and refracted beams.

By considering two infinitesimally close paths separating two points located in the same medium one can easily see that an identical equation holds for the reflected beam wavevector of components $k_{x,r}$ and $k_{y,r}$.

Without loss of generality, we choose the coordinate system such that $\vec{k}_i$ lies in the yz-plane, that is, $k_{x,i} = 0$. Equation 2 shows that a phase gradient with a component oriented along the x-direction leads to an x-component for both $\vec{k}_r$ and $\vec{k}_t$. It is therefore no longer possible to define a plane that contains the incident, the reflected and the transmitted beams. The usual planar k-space representation used to illustrate refraction and reflection needs to be extended into three dimensions (as depicted in Figure 1b)). The reflection (refraction) angles are now given by the direction of the wavevector which intersects the k-sphere in the medium 1 (2) of radius $k = k_0 n$ where n is the refractive index, while satisfying the tangential wavevector relation (eq 2). A schematic of this new physical situation is presented in Figure 1b,c. This 3D geometrical k-space representation is widely used to describe electron, neutron and X-ray diffraction and is known in the literature as Ewald's sphere.[28]

The directions of the reflected and refracted wavevectors are characterized by the angles $\vartheta_{r(t)}$ (the angle between $\vec{k}_{r(t)}$ and its projection on the xz-plane) and $\varphi_{r(t)}$ (the angle formed by the projection of $\vec{k}_{r(t)}$ on the xz-plane and the z-axis) as defined in Figure 1b). With this choice of notation, any wavevector $\vec{k}$ can be decomposed as follow

$$\begin{cases} k_x = k \cos\vartheta \sin\varphi \\ k_y = k \sin\vartheta \\ k_z = \sqrt{k^2 - (k_x{}^2 + k_y{}^2)} = k \cos\vartheta \cos\varphi \end{cases} \quad (3)$$

Substituing eq 3 in eq 2, we obtain the generalized reflection and refraction laws in three dimensions. The reflection of light in 3D at an interface with phase gradient is then given by

$$\begin{cases} \cos\vartheta_r \sin\varphi_r = \dfrac{1}{n_i k_0}\dfrac{d\Phi}{dx} \\ \sin\vartheta_r - \sin\vartheta_i = \dfrac{1}{n_i k_0}\dfrac{d\Phi}{dy} \end{cases} \quad (4)$$

dx.doi.org/10.1021/nl300204s | Nano Lett. 2012, 12, 1702−1706

For refraction, the 3D Snell's law is given by

$$\begin{cases} \cos\vartheta_t \sin\varphi_t = \dfrac{1}{n_t k_0}\dfrac{d\Phi}{dx} \\ n_t \sin\vartheta_t - n_i \sin\vartheta_i = \dfrac{1}{k_0}\dfrac{d\Phi}{dy} \end{cases} \quad (5)$$

Note that when the phase gradient is oriented along the plane of incidence ($d\Phi/dx = 0$) the anomalous reflection and refraction are in plane. Equations 3 and 4 lead to the new critical angles for reflection and refraction previously presented for the case of in plane reflection and refraction.[21] The nonlinear nature of these equations is such that two different critical angles now exist for both reflection and refraction (see Supporting Information).

In the following, we present the experimental observation of out-of-plane refraction in accordance with the new 3D law (eq 5) using an interface patterned with an array of optical antennas.[12,13] By suitably designing their geometry one can easily control the phase and amplitude of light scattered by each antenna to generate the desired wavefront. We note that the choice of the optical resonators is potentially wide and includes nanocrystals,[29] electromagnetic cavities[30,31] and nanoparticles clusters.[32,33] For convenience, we have used the broadband V-shaped plasmonic antennas arrays used in our previous experiments[21] and oriented them in such a way that the interface phase gradient forms an angle α with respect to the plane of incidence (Figure 2).

Note that although the anomalous beams generated by the interface are cross-polarized with respect to the incident beam (see the simulations in the Supporting Information), Fermat's principle of stationary phase can still be applied because the polarization conversion at the antennas is a coherent process. The predicted angles of generalized refraction given by eq 5 are directly compared with the experimental values.

Figure 3a is an example of the experimental far field for a phase gradient oriented in the direction perpendicular to the plane of incidence, which confirms out-of-plane refraction. In spite of the array periodicity, the effect is markedly different from light scattering in conventional gratings, where pairs of diffraction orders are generated symmetrically with respect to the zeroth order. Our array behaves functionally as a blazed grating[1] where light is preferentially diffracted into a single direction, an effect previously demonstrated for phase gradients contained in the plane of incidence ($\alpha = 0°$).[21] We have now verified both experimentally and numerically that this also holds true for noncoplanar refraction (Figure S2, Supporting Information). However there is a critical difference in the way the phase of the scattered light is controlled in our array compared to a blazed grating, due to major structural differences. In the latter it is governed by optical path differences between light scattered by the grating grooves, that is by a propagation effect, whereas in our optically thin plasmonic interface, it is controlled by abrupt phase shifts (phase discontinuities) since light scatters off deep sub-wavelength thick optical antennas.[21] To validate the predictions of the 3D Snell's law (eq 5), we performed an experimental study of both the ordinarily and anomalously refracted angles for various incidence angles ϑ_i and various phase gradient orientations (α angles). The magnitude of the phase gradient is fixed to $d\Phi/dr = (2\pi)/(15\ \mu m)$ for all the experiments. The results are summarized in Figure 3b and unambiguously show

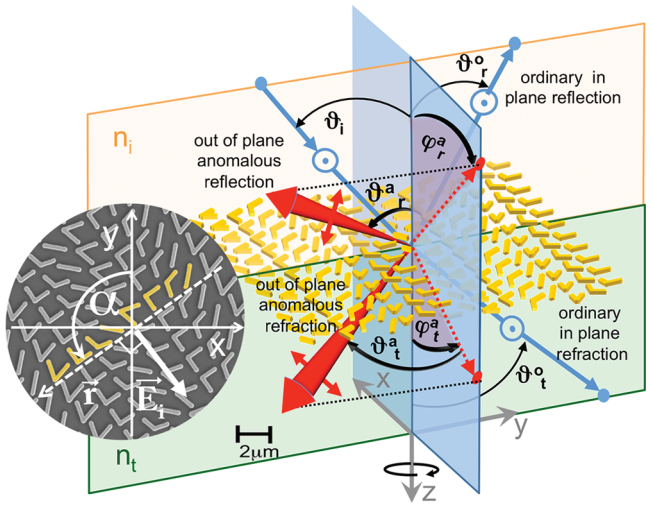

Figure 2. Schematic representation of the reflection and refraction of light in 3D. The incident light generated by a quantum cascade laser (λ = 8 μm) impinges at an angle ϑ_i with respect to the z-axis on the interface that separates two media. The interface (xy-plane at $z = 0$) is between silicon (Si, refractive index $n_i = 3.41$) and air ($n_t = 1$) and light is incident from the Si side. The sample is created by periodically translating in the x–y plane the unit cell consisting of 8 subwavelength V-shaped antennas (colored in yellow in the inset scanning electron microscope image). As described in ref 21 part of the light is reflected and refracted according to the standard laws in the same polarization as the incident beam. We call ϑ_r^o and ϑ_t^o the corresponding reflection and refraction angles. Anomalously reflected and refracted beams are also generated, described by eq 4 and 5, which are cross polarized with respect to the incident beam. The array imposes a linear phase gradient at the interface in the direction $\vec{r}$ that forms an angle α with the y-axis as shown in the inset. For $\alpha = m\pi$ ($m = 0, \pm1,...$), the phase gradient is exclusively oriented along y and so the interface scatters the cross polarized light exclusively in the plane of incidence. For α not satisfting the above equality, a component of the phase gradient out of the plane of incidence is created, resulting in out of the plane anomalous reflection and refraction. The V-shaped antennas support two orthogonal modes of current oscillation.[21] The antennas were designed such that they need to be excited with a linear state of polarization at an angle of 45° with respect to the two antenna modes in order for the polarization of the anomalous beams to be orthogonal to that of the incident beams. To maintain this configuration when the sample is rotated, we simultaneously rotated the incident polarization. The direction of the outgoing anomalous beams, which is determined by the new parallel wavevector conservation law (eq 2), is now given by two angles, ϑ_r^a (ϑ_t^a) and $\varphi_r^a(\varphi_t^a)$ describing anomalous reflection (refraction).

that out of plane refraction is observed. It also shows that the phase gradient orientation changes the out-of-plane refraction angles accordingly to eq 5. It is worth noticing that regardless of the different orientations of the phase gradient, the ordinary refracted beam always lies in the plane of incidence, at angles predicted by the textbook Snell's law.

We note that effect of the optically thin array of antennas on the propagating light beam is described by a phase discontinuity $\Phi(r)$ with a constant gradient along the interface, assumed to be a continuous function of r. This model treats the interface as continuous medium which imparts a phase gradient to the wavefront, accounting for the interaction with the optical antennas and allowing a simple analytical derivation of anomalous refraction and reflection in 3D. The validity of this approach is confirmed by excellent agreement with full wave 3D simulations.

dx.doi.org/10.1021/nl300204s | Nano Lett. 2012, 12, 1702–1706

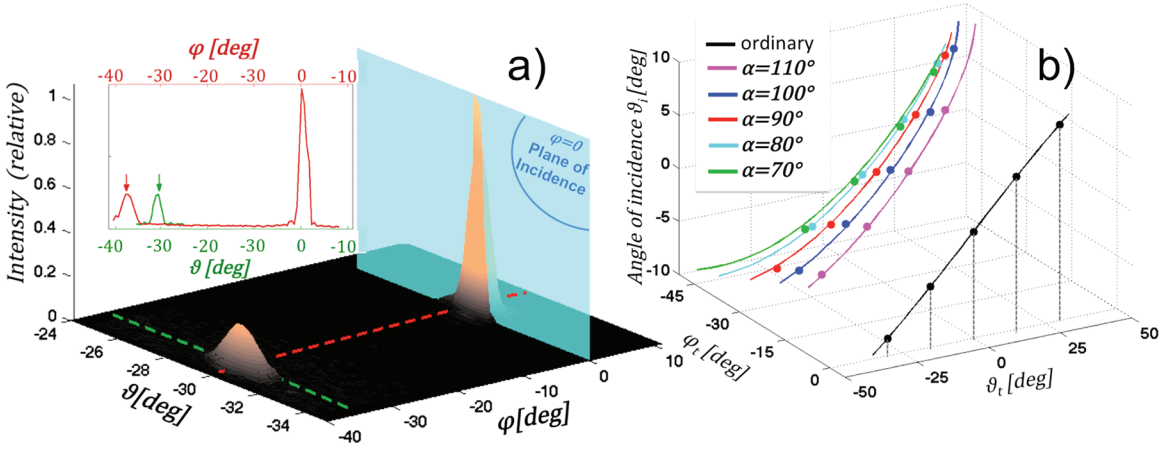

Figure 3. Experimental observation of out-of-plane refraction. (a) Measured far-field intensity as a function of the angular position of the detector ϑ and φ (defined in a similar way as ϑ_t and φ_t in Figure 1) for a laser beam incident on the interface from the silicon side at an angle $\vartheta_i = -8.45°$ and for a phase gradient perpendicular to the plane of incidence ($\alpha = 90°$). As expected, the ordinary refracted beam is in plane ($\varphi = 0°$) at an angle following the conventional Snell's law, that is, $\vartheta = -30°$. The anomalous beam is refracted out of plane at an angle $\varphi = -38°$ and $\vartheta = -30°$. Dark colors correspond to low intensities. The divergence angle of both the ordinary and the anomalous beams is related to the spot size of the beam focused on the sample to create a flat incident wavefront. The inset shows the angular distribution of the intensity at a fixed $\varphi = -38°$ (green curve) and at a fixed $\vartheta = -30°$ (red curve). The experimental setup working in the mid-infrared spectral region with bulky detector did not allow us to monitor the reflection peaks for most of the phase gradient orientation angles α (see Supporting Information). (b) Angles of refraction versus angles of incidence and phase gradients orientation α. The black line is the theoretical curve from the classical Snell law. Colored lines are theoretical curves from the 3D Snell law (eq 5) for different phase gradient orientations. Circles are experimental data.

In conclusion, we have derived generalized reflection and refraction laws in 3D that account for any orientation of phase discontinuity gradients at an interface and we have used plasmonic interfaces to demonstrate experimentally off-plane refraction and its wide tunability by varying the orientation of the plane of incidence with respect to the antenna array.

We expect that the phase control made possible by suitably designed optical antenna arrays will lead to the development of a new class of flat optical components such as planar lenses with high numerical aperture, flat polarization converters and flat vortex plates[23] including optical phased arrays.

Methods. *V-Shaped Optical Antennas As Phase Elements.* Phase discontinuities are achieved by considering the scattering from V-shaped plasmonic antennas, that is, gold antennas made of two arms of equal length h connected at one end at an angle. We designed a set of eight elements that produce phase shifts of the incident wavefront in the range from 0 to 2π. Full control of the phase is achieved by using the symmetric and antisymmetric modes of the V-shaped antennas.[21] This property allows one to adjust the scattering amplitude of each element to be equal so that the interface only modifies the phase of the beam without amplitude modulation. A two-dimensional antenna array is constructed by periodically arranging a unit cell comprising the eight elements. The gold V-antenna array, 230 μm × 230 μm in size, was fabricated using electron-beam lithography on 280 μm thick intrinsic silicon wafers. The thickness of gold is 50 and 10 nm titanium is used as the adhesion layer. The width of the antenna arms is ∼220 nm.

Experimental Setup and Measurements. A buried-heterostructure quantum cascade laser (QCL) with central wavelength 8 μm and spectral width ∼0.2 μm was used as the light source in the experiments. It impinges on the sample at an angle ϑ_i with respect to the z-axis, in the yz-plane. The QCL was operated in pulsed mode with a 1.5 μs pulse width and 80 kHz repetition rate at room temperature and the average output power is about 5 mW. A 1 in. diameter zinc selenide (ZnSe) lens with one-inch focal length was used to collimate the emission from the QCL and another 1 in. diameter ZnSe lens with 20 in. focal length was used to focus the laser beam on the antenna array. The beam waist w_0 on the sample is ∼100 μm (w_0 is the radius at which the field amplitude drops to $1/e$ of the peak value), and the Rayleigh length of the Gaussian beam is ∼4 mm. This ensures that the whole antenna array is illuminated by a plane-wave-like excitation. The laser beam was incident from the backside of the silicon wafer, which is not decorated with antennas. The transmitted signal was recorded by a mercury−cadmium−telluride (MCT) detector mounted on a double motorized rotation stage to scan the two-dimensional far-field. Because the MCT detector is mounted in a cooled enclosure, its size prevents the measurement of anomalous reflection. For simplicity, we fix the phase gradient to a constant value $d\Phi/dr = (2\pi)/(15\ \mu m))$ and change its projections along the x- and y-direction by simply rotating the interface around its normal axis (angle α), as depicted in inset Figure 2.

■ ASSOCIATED CONTENT

Ⓢ Supporting Information

Detailed simulation information, additional figures and equations. This material is available free of charge via the Internet at http://pubs.acs.org.

■ AUTHOR INFORMATION

Corresponding Author

*E-mail: capasso@seas.harvard.edu.

Notes

The authors declare no competing financial interest.

■ ACKNOWLEDGMENTS

We thank J. Lin and R. Blanchard for helpful discussions. This work was supported in part by the Defense Advanced Research Projects Agency (DARPA) N/MEMS S&T Fundamentals

program under Grant N66001-10-1-4008 issued by the Space and Naval Warfare Systems Center Pacific (SPAWAR). The authors acknowledge support from the National Science Foundation, Harvard Nanoscale Science and Engineering Center (NSEC) under contract NSF/PHY 06-46094, and the Center for Nanoscale Systems (CNS) at Harvard University. P.G acknowledges funding from the Robert A. Welch Foundation (A-1261). Z.G. acknowledges funding from the European Communities Seventh Framework Programme (FP7/2007-2013) under Grant PIOF-GA-2009-235860. M.A.K. is supported by the National Science Foundation through a Graduate Research Fellowship. Harvard CNS is a member of the National Nanotechnology Infrastructure Network (NNIN).

REFERENCES

(1) Hecht, E. *Optics*, 3rd ed.; Addison Wesley Publishing Company: Reading, MA, 1997.
(2) Born, M.; Wolf, E. *Principles of Optic*, 7th ed.; Cambridge University Press: New York, 1999.
(3) Griffiths, D. J. *Introduction to electrodynamics*, 3rd ed.; Addison Wesley Publishing Company: Reading, MA 1999.
(4) Feynman, R. P.; Hibbs, A. R. *Quantum Mechanics and Path Integrals*; McGraw-Hill: New York, 1965.
(5) Veselago, V. G. *Sov. Phys. Usp.* **1968**, *10*, 509−514.
(6) Pendry, J. B. *Phys. Rev. Lett.* **2000**, *85*, 3966−3969.
(7) Pendry, J. B.; Schurig, D.; Smith, D. R. *Science* **2006**, *312*, 1780−1782.
(8) Cai, W.; Shalaev, V. *Optical metamaterials: Fundamentals and applications*; Springer: New York, 2009.
(9) Shelby, R. A.; Smith, D. R.; Schultz, S. *Science* **2001**, *292*, 77−79.
(10) Parazzoli, C. G.; Greegor, R. B.; Li, K.; Koltenbah, B. E. C.; Tanielian, M. *Phys. Rev. Lett.* **2003**, *90*, 107401.
(11) Houck, A. A.; Brock, J. B.; Chuang, I. L. *Phys. Rev. Lett.* **2003**, *90*, 137401.
(12) Grober, R. D.; Schoelkopf, R. J.; Prober, D. E. *Appl. Phys. Lett.* **1997**, *70*, 1354−1356.
(13) Novotny, L.; Van Hulst, N. *Nat. Photonics* **2011**, *5*, 83−90.
(14) Wedge, S.; Wasey, J. A. E.; Barnes, W. L. *Appl. Phys. Lett.* **2004**, *85*, 182.
(15) Yu, N.; Wang, Q; Capasso, F. *Laser Photonics Rev.* **2012**, *6*, 24−46.
(16) Zhao, Y.; Alù, A. *Phys. Rev. B* **2011**, *84*, 205428.
(17) Novotny, L.; Stranick, S. J. *Annu. Rev. Phys. Chem.* **2006**, *57*, 303−331.
(18) Cubukcu, E.; Yu, N.; Smythe, E. J.; Diehl, L.; Crozier, K. B.; Capasso, F. *IEEE J. Sel. Top. Quant. Electron.* **2008**, *14*, 1448−1461.
(19) Boriskina, S. V.; Povinelli, M.; Astratov, V. N.; Zayats, A. V.; Podolskiy, V. A. *Opt. Express* **2011**, *19*, 2204−2208.
(20) Dal Negro, L.; Boriskina, S. V. *Laser Photonics Rev.* **2011**, 1−41.
(21) Yu, N.; Genevet, P.; Kats, M. A.; Aieta, F.; Tetienne, J. P.; Capasso, F.; Gaburro, Z. *Science* **2011**, *334*, 333−337 .
(22) Engheta, N. *Science* **2011**, *334*, 317−318.
(23) Genevet, P.; Yu, N.; Aieta, F.; Lin, J.; Kats, M. A.; Blanchard, R.; Scully, M. O.; Gaburro, Z.; Capasso, F. *Appl. Phys. Lett.* **2012**, *100*, 013101.
(24) Ni, X.; Emani, N. K.; Kildishev, A. V.; Boltasseva, A.; Shalaev, V. M. *Science* **2012**, *335*, 427.
(25) Dupertuis, M. A.; Proctor, M.; Acklin, B. *J. Opt. Soc. Am. A* **1994**, *11*, 1159−1166.
(26) Kosaka, H.; Kawashima, T.; Tomita, A.; Notomi, M.; Tamamaura, T.; Sato, T.; Kawakami, S. *Phys. Rev. B* **1998**, *58*, 16.
(27) Prasad, T.; Colvin, V.; Mittleman, D. *Phys. Rev. B* **2003**, *67*, 165103.
(28) Ewald, P. P. *Acta Crystallogr., Sect. A* **1969**, *25*, 103−108.
(29) Norris, D. J.; Efros, A. L.; Erwin, S. C. *Science* **2008**, *319*, 1776−1779.
(30) Miyazaki, H. T.; Kurokawa, Y. *Appl. Phys. Lett.* **2006**, *89*, 211126.
(31) Fattal, D.; Li, J.; Peng, Z.; Fiorentino, M.; Beausoleil, R. G. *Nat. Photonics* **2010**, *4*, 466−470.
(32) Fan, J. A.; et al. *Science* **2010**, *328*, 1135−1138.
(33) Luk'yanchuk, B; et al. *Nat. Mater.* **2010**, *9*, 707−715.